Biotechnology and Bioengineering, April 2009, Volume 102, Issue 5, Pages 1505-1512

DBT degradation enhancement by decorating *Rhodococcus erythropolis* IGST8 with magnetic Fe_3O_4 nanoparticles

Farahnaz Ansari[1]*, Pavel Grigoriev[2], Susan Libor[1], Ibtisam E. Tothill[3] and Jeremy J. Ramsden[1]

[1] *Microsystems & Nanotechnology Centre, Cranfield University, Bedfordshire, MK43 0AL, UK*

[2]*Institute of Cell Biophysics, Russian Academy of Science, Pushchino, Moscow Region, 142290, Russia*

[3]*Cranfield Health, Cranfield University, Bedfordshire, MK43 0AL, UK*

* Corresponding author: Farahnaz Ansari

Address: *Microsystems & Nanotechnology Centre, Cranfield University, Bedfordshire, MK43 0AL, UK*

Tel.: +44 (0)1234 750111 ext 2465;

fax: +44(0) 751346.

E-mail address: f.ansari@cranfield.ac.uk

Keywords: biodesulfurization; dibenzothiophene; *Rhodococcus erythropolis*; magnetic Fe_3O_4; nanoparticles, black lipid membrane

Abstract

Biodesulfurization (BDS) of dibenzothiophene (DBT) was carried out by *Rhodococcus erythropolis* IGST8 decorated with magnetic Fe_3O_4 nanoparticles, synthesized in-house by a chemical method, with an average size of 45–50 nm, in order to facilitate the post-reaction separation of the bacteria from the reaction mixture. Scanning electron microscopy (SEM) showed that the magnetic nanoparticles substantially coated the surfaces of the bacteria. It was found that the decorated cells had a 56% higher DBT desulfurization activity in basic salt medium (BSM) compared to the nondecorated cells. We propose that this is due to permeabilization of the bacterial membrane, facilitating the entry and exit of reactant and product respectively. Model experiments with black lipid membranes (BLM) demonstrated that the nanoparticles indeed enhance membrane permeability.

1. Introduction

In any industrial process using freely dispersed microorganisms as catalysts, they need to be separated from the products after catalysis has taken place and the reaction has reached its conclusion. Typically, the separation is carried out either by filtration or centrifugation (Luo and Sirkar, 2000). This is the first step of the downstream processes required to purify the product.

Although the free dispersal of microorganisms in a fluid reaction volume optimizes mass transport, it is sometimes difficult to carry out the necessary separation afterwards, and usually the separation procedure compromises viability, i.e. the organisms die. Therefore, efforts have been made to immobilize bacteria, typically in the form of biofilms coating

reaction vessels with high surface to volume ratios[1]. The starting materials must then simply be made to flow over the biofilm, and no separation is subsequently required (Naito et al., 2001). Furthermore, biofilms offer protection to the cells against adverse environmental conditions, and to some extent at least they are self-renewing and may therefore be used for many production cycles, or even for continuous rather than batch processes. On the other hand, mass transport is much slower than with freely dispersed microorganisms.

Some DBT biodesulfurization results have been reported using immobilized *Rhodococcus erythropolis*. Naito et al. (2001) immobilized the bacteria by entrapping them with calcium alginate, agar and resin polymers; and Prieto et al. (2002) used Biolite beads to support an adsorbed network of bacteria on their external surface. Naito et al. (2001) found out that using immobilized cells made it easy to recover desulfurized oil and to use the biocatalyst repeatedly for long periods with reactivation. Immobilization of bacteria by traditional entrapment methods has major downsides, however. Mass transfer problems reduce cell access to the substrate and usually lead to a disappointingly low biotransformation activity (Xu et al., 2006)[2].

In order to combine the advantages of immobilization—i.e. ease of separation and microbial longevity—with those of free diffusion—i.e. good mass transport—another approach is

[1] Three major techniques are used for immobilizing bacteria: entrapment, adsorption and coupling (Corcoran, 1985). To achieve entrapment, the microbial cells are mixed with a gel-forming polymer, yielding pores smaller than the size of the cells. This ensures retention of the cells, but permits movement of nutrients, starting reagents and products. Adsorption means allowing the bacteria to form weak chemical bonds to the substrate; electrostatic interactions between a charged support and charged cells have been made use of (Yang and Albayrak, 2006). However, the forces involved in cell attachment are then so weak that cells are readily lost from the adsorbent (Shan et al., 2005). To overcome this problem, cells can be covalently bonded (coupled) to an activated support (Hulst and Trumper, 1989).

[2] As an exception to the general rule, Díaz et al. (2002) reported that by immobilization of bacterial cells the biodegradation rate of crude oil was significantly enhanced compared to free-living cells.

possible, namely to decorate the bacterial cells with magnetic nanoparticles (Shan et al., 2005). After completion of the reaction, the bacterial cells can be separated from the products using a magnetic field. This is a much milder and more cost-effective process than centrifugation, and allows the bacteria to be reused many times (Gupta and Hung, 1989).

In the present work we have made use of a widely studied Gram-positive desulfurizing bacterial strain, *Rhodococcus erythropolis* IGTS8, in order to investigate the effects of decorating the bacteria with magnetic nanoparticles. *R. erythropolis* is known to be able to utilize a wide variety of sulfur compounds as sulfur sources (Kayser et al., 1993) and this microorganism has been investigated in some detail (Gray et al., 1996; Li et al., 1996; Ansari et al., 2007). We suspended *R. erythropolis* in basic salt medium (BSM) containing dibenzothiophene (DBT) as the sole source of sulfur, and the DBT degradation ability of *R. erythropolis* was measured with the help of HPLC. DBT was chosen in this study as a model compound for the forms of thiophenic sulfur found in fossil fuels; up to 70% of the sulfur in petroleum is found as DBT and substituted DBTs (methylated DBTs); these compounds are however particularly recalcitrant to hydrodesulfurization (HDS), the current standard industrial method (Yang and Marison, 2005). We have used Fe_3O_4 as the nanoparticulate material; it is chemically stable in the working environment and nontoxic to the bacterium. Previous work by Yang and Albayrak (2006) has moreover suggested that bacteria can be decorated with them by simple adsorption.

2. Experimental

2.1 Chemicals

Dibenzothiophene (DBT) (99%), dimethyl sulfoxide, 2-hydroxybiphenyl (HBP), ferrous chloride tetrahydrate ($FeCl_2 \cdot 4H_2O$), ferric chloride hexahydrate ($FeCl_3 \cdot 6H_2O$), glycine, Ringer's solution and all other chemicals were from Fisher Scientific (UK), Lipids were from Sigma, Water was purified by ion exchange and reverse osmosis (ELGA-option3B, Elga Water Ltd, UK).

2.2 Bacterial strain and medium

Rhodococcus erythropolis IGTS8 (ATCC 53968) was from American Type Culture Collections. The bacteria were grown in basic salt medium (BSM), a sulfur-free medium containing 2.44 g KH_2PO_4, 5.47 g Na_2HPO_4, 2.00 g NH_4Cl, 0.2 g $MgCl_2 \cdot 6H_2O$, 0.001 g $CaCl_2 \cdot 2H_2O$, 0.001 g $FeCl_3 \cdot 6H_2O$, 0.004 g $MnCl_2 \cdot 4H_2O$ and 1.84 g glycerol in 1 L of deionized water. DBT dissolved in ethanol was added to give a final concentration of 0.5 mM as the sole sulfur source.

2.3 Nanoparticle synthesis

Magnetic nanoparticles were synthesized using the procedure described by Yeh et al., (2004) to obtain Fe_3O_4 nanoparticles: briefly 25 mL of 0.2 M ferrous chloride ($FeCl_2$) was mixed with 100 mL of 0.1 M ferric chloride ($FeCl_3$) solution in a flask at room temperature and then 3 mL of 2 M HCl solution was added to make the solution slightly acidic. Then 1 g of glycine was added, and 11 mL 5 M NaOH solution was slowly dripped into the mixture to increase its pH to over 10, to provide an alkaline environment for Fe_3O_4 to precipitate; next, an additional 3 g of glycine was added, and the mixture agitated with an FB15024 vortexer

(Topmix, UK) for 10–15 min and then sonicated for 30 min; subsequently 5 mL acetone was added and agitated. The resulting precipitate (Fe_3O_4) was isolated with a permanent magnet and the supernatant discarded by decantation. The precipitate was washed twice with ultrapure water followed by centrifugation at 2500 *g* for 5 min to remove excess ions in the suspension and obtain water-dispersible nanoparticles. Finally, the washed precipitate was dispersed in ultrapure water for further investigation. The magnetic nanoparticle concentration is expressed as dry weight per volume of suspension medium.

A particle diameter of 50 nm was chosen, because if the particles are large, their Brownian energy overwhelms the relatively weak attachment forces. Preliminary experiments using iron oxide particles with a diameter of 1 μm (Dynabeads, Dynal Biotech) showed that they did not attach to the bacteria. Furthermore, the particles should be small enough to be superparamagnetic, i.e. smaller than the critical magnetic domain size (Morrish et al., 1956; Schmidt 2001; Zhang et al., 2006). This critical diameter is around 50 nm for our material.

2.4 Nanoparticle characterization

Transmission electron microscopy (TEM) and scanning electron microscopy (SEM) were used to characterize the particles (Fig.1). In order to prepare TEM samples, the final nanoparticle slurry was sonicated for approximately 5 min to better disperse the nanoparticles. A drop was placed with a carbon-coated copper TEM grid (200–300 mesh) and then left to dry in air. The particle diameters were determined directly from the TEM images to be in the range of 45–55 nm (Fig.1A).

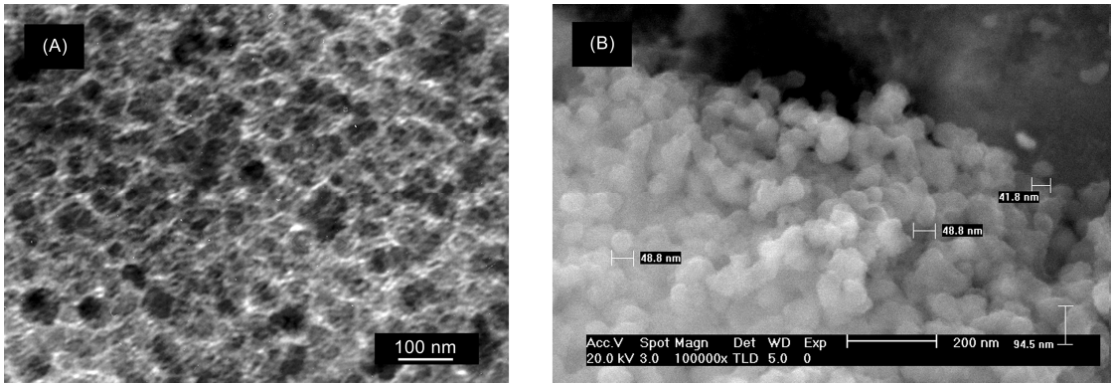

Fig.1. (A) TEM image of the Fe_3O_4 nanoparticles. Capillary forces during drying of the suspension on the grid result in the aggregation visible on the micrographs. (B) SEM image of the synthesized Fe_3O_4 nanoparticles.

Fig. 2 shows a bar chart of the sizes. Further characterization of the synthesised Fe_3O_4 nanoparticles was obtained using a FEI XL30 field emission SEM (Fig.1B). In order to prepare SEM samples, the particle suspension was washed several times in deionized water to remove any salt residue, then diluted using deionized water, and finally using a pipette a drop was placed on an Al-stub and left to dry overnight, before mounting the stub on the SEM sample holder. The operating voltage was in the range of 10–20 kV to minimize charging of the sample. The SEM image were not subjected to quantitative analysis, but merely served to gain a visual impression.

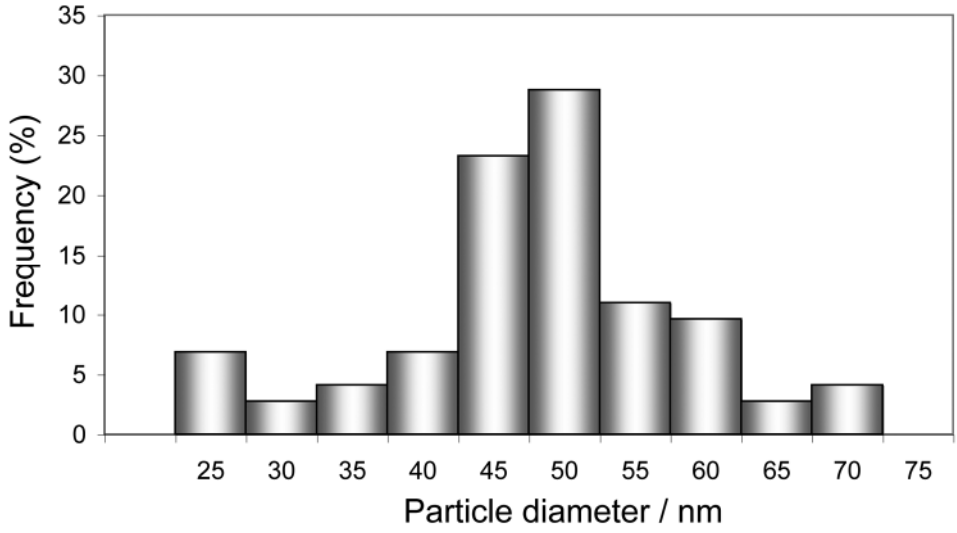

Fig. 2. Bar chart of the particle sizes from a typical preparation determined from TEM images (a total of 100 particles were measured). Mean size is 47.22 ± 0.96 nm (S.d.)

Magnetic hysteresis loops of the samples were measured using a Magnetic Measurements (Peterson Instruments, UK) variable field translation balance (MMVFTB). Saturation magnetization (9.9 emu/g) was obtained from the hysteresis loop resulting from applying a magnetic field from -8 to +8 kOe (Fig. 3). The paramagnetic component was removed by assessing the gradient of the magnetization curve (B vs H) once saturation had been reached. It should be emphasized that the residual magnetization is almost negligible for these particles, which is very likely important for achiving good dispersibility of the nanoparticles in a fluid.

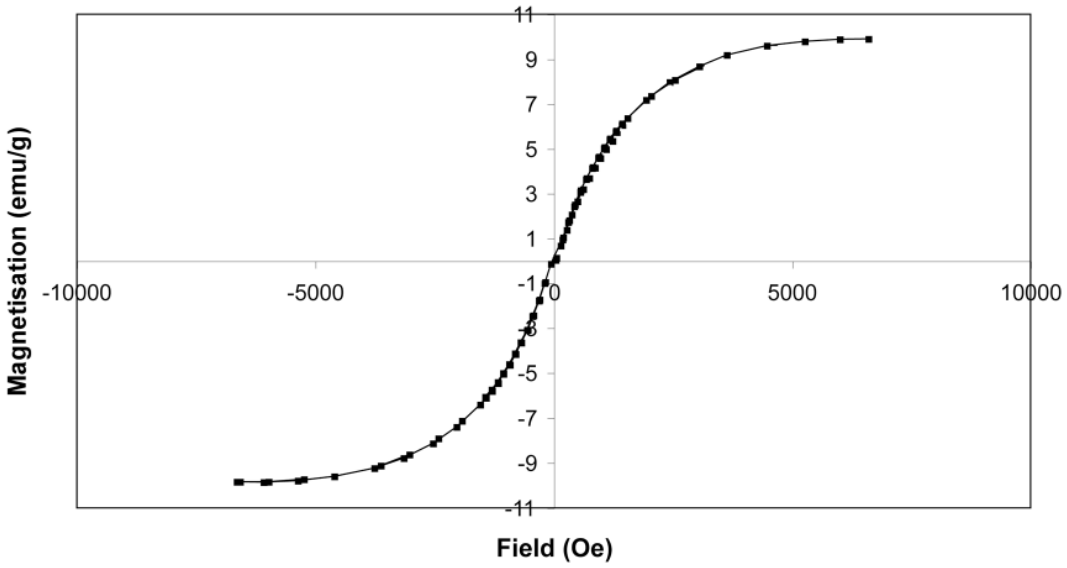

Fig.3. Magnetic hysteresis loop of the Fe_3O_4 nanoparticles measured at room temperature. The paramagnetic component of the magnetization has been removed according to a standard procedure.

Powder X-ray diffraction (XRD) studies were performed between 10° and 85° with a copper X-ray source (Siemens). The XRD pattern of the nanoparticles indicates the presence of predominantly Fe_3O_4 crystals (Fig. 4).

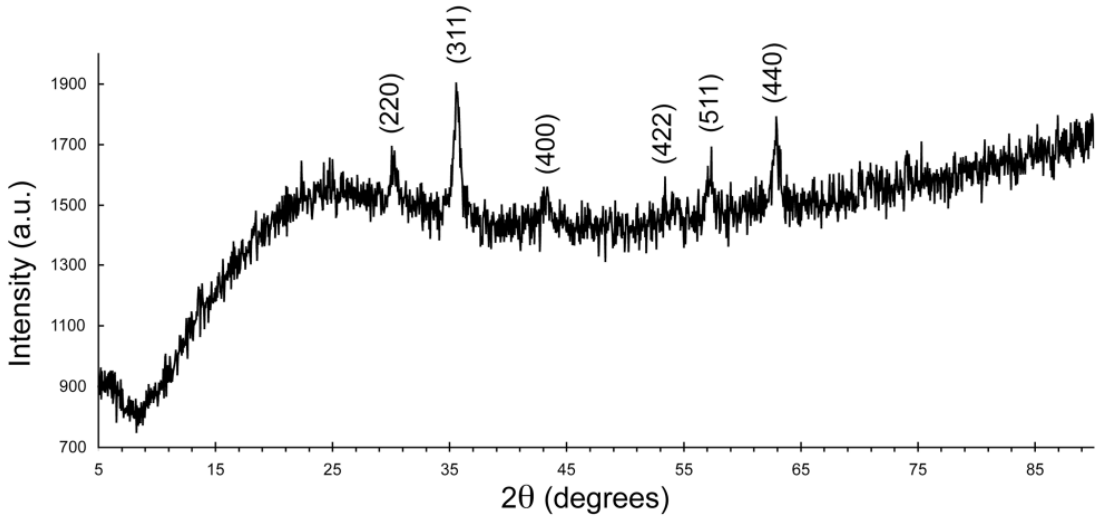

Fig.4. X-ray diffraction pattern of the nanoparticles. The numbers in parenthesis give the Miller indices of pure Fe_3O_4 (NBS, 1976) assigned to the observed peaks.

The zeta potentials of the prepared nanoparticles suspended in deionized water (100 μg/mL) were measured using a 3000HS Zetasizer (Malvern Instruments Ltd, UK).

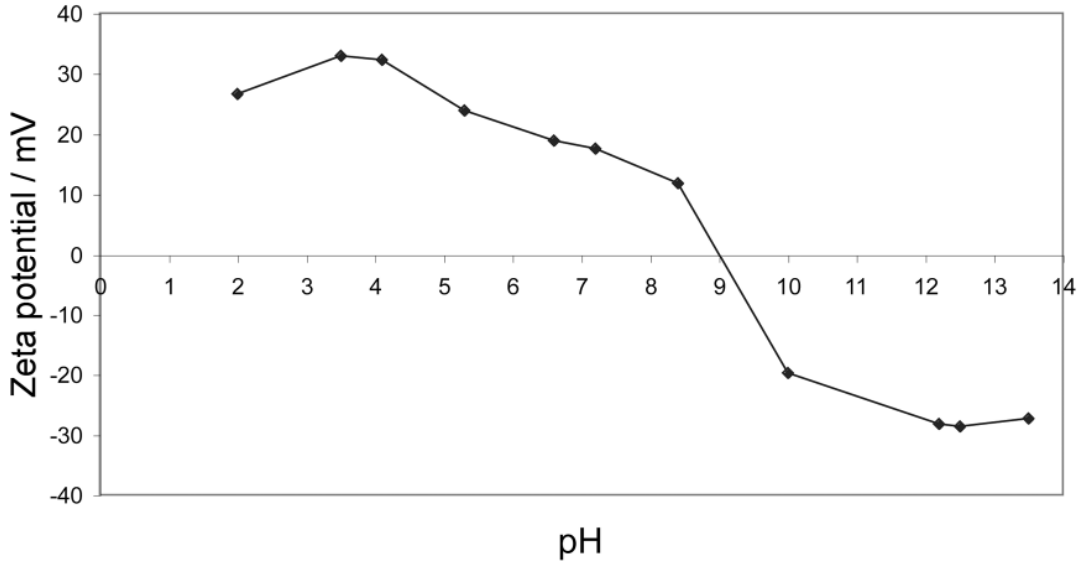

Fig.5. Surface charges of the Fe_3O_4 magnetic nanoparticles suspended in water at 25 °C as a function of pH, changed by appropriate additions of 2 M HCl or NaOH.

The pH of the as-prepared particles in suspension was 7.0 ± 0.2. The variation of the zeta potential with pH (Fig. 5) revealed that the isoelectric point of the particles is 9.0. Hence at pH 7, at which the bacteria are negatively charged, they will electrostatically attract the nanoparticles.

2.5 *Cell growth and decoration*

The bacteria were grown in BSM until the mid-exponential growth phase and harvested by centrifugation at 1400 *g* for 10 min. The cell pellets were washed twice with Ringer's solution and resuspended back in BSM at a concentration of 5.6 mg dry cells/L. The cells were then decorated with magnetic nanoparticles as follows: 10 mL of a suspension

containing 100 µg/mL Fe_3O_4 nanoparticles per mL of water were mixed with 100 mL of the cell suspension in BSM at a final concentration of 0.5 mM. The ratio of nanoparticle mass to biomass is 1.78 w/w. We estimated that this ratio makes sufficient particles available per bacterium to yield a suitable level of decoration. The resulting successful separation (Fig. 6) did not require subsequent optimization.

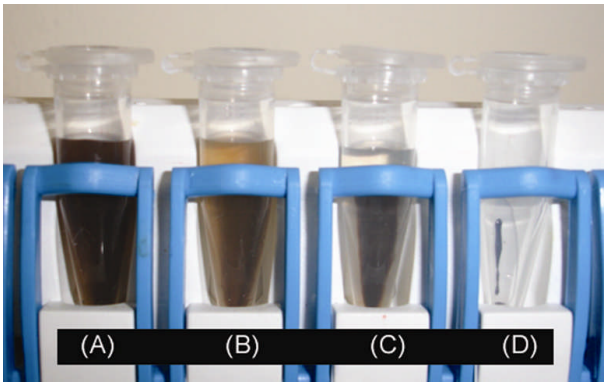

Fig.6. Photograph of nanoparticle-coated cells (*Rhodococcus erythropolis* IGTS8) in Eppendorf tubes showing, successively: (A) dispersed cells coated with magnetic nanoparticles; (B and C) coated cells were gradually concentrated and collected towards the rear of the tube by an external permanent magnet (within the white housing behind the tubes); (D) liquid medium free of suspended nanoparticles, which are visible as a thin dark stripe at the back of the tube.

2.6 Batch biodesulfurization of DBT

Biodesulfurization was carried out using the cells in 100 mL of BSM containing DBT at a final concentration of 0.5 mM, in a 250 mL flask incubated on a rotary shaker at 120 rpm and 30 ºC (0.5 mM of DBT are equivalent to 0.092 g DBT/L). For analysis of the supernatant by HPLC, it should not contain any contamination (like free bacteria or other nonmagnetic contamination) that would damage the HPLC column. Therefore, prior to analysing the

supernatant, the cells were separated from the reaction mixture by centrifugation at 6600 *g* for 10 min, so that the same procedure could be used for both decorated & nondecorated controls.

2.7 Product analysis

The concentrations of DBT and HBP were analyzed by high-performance liquid chromatography (HPLC) using a HPLC Model LC-10AD VP (Shimadzu) equipped with a Nova Pak phenyl column (3.9×150 mm) with a guard column. Isocratic elution with 60% acetonitrile and 40% water at 1.5 mL min^{-1} was carried out and detection was realized with a 117 UV detector fixed at a wavelength of 233 nm. The mobile phase, a mixture of HPLC grade water and acetonitrile, was sonicated for 10 min, and further deaerated with helium before use.

2.8 Nanoparticle-induced membrane permeability assay

Lipid bilayer membranes were formed by the method of Mueller et al. (1962) from a cardiolipids:phosphatidylcholine 5:95 mixture mimicking the bacterial outer membrane. The membrane current was measured by an OPA 129 operational amplifier (Burr-Brown) used as a current-to-voltage converter.

3. Results

3.1 Visualization of decoration

Scanning electron micrographs of the surfaces of cells decorated with Fe_3O_4 nanoparticles are shown in Fig. 7, which clearly shows that the Fe_3O_4 nanoparticles were adsorbed on the surface of the bacteria.

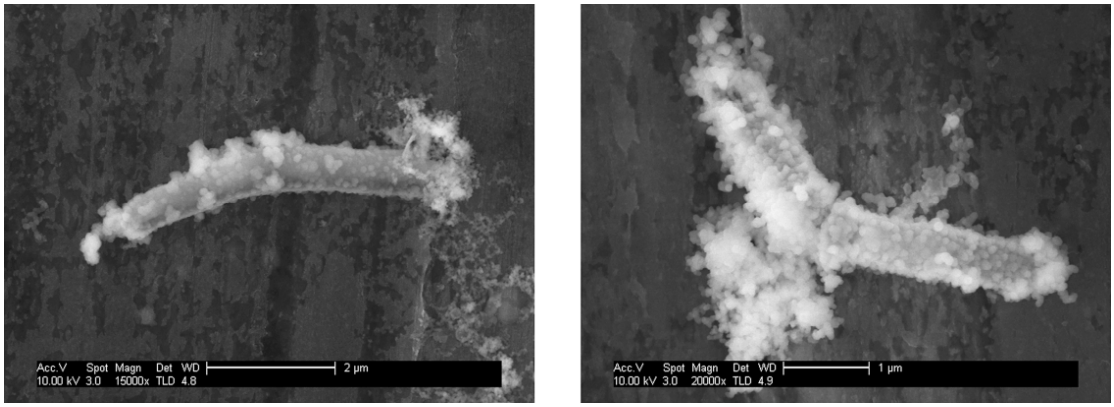

Fig.7. SEM images of two different *Rhodococcus erythropolis* IGTS8 bacteria decorated with magnetic nanoparticles. The bacterium shown on the right panel is about to undergo division.

3.2 Magnetic separation

Fig. 6 shows a suspension of bacteria coated by nanoparticles in a holder equipped with a removable slide-out magnet: the decorated cells in the liquid culture medium could easily be separated by bringing an external magnet into their vicinity.

3.3 Biodesulfurization

Fig. 8 compares the degradation of DBT with nondecorated and nanoparticle-coated cells. The results show that the production of HBP was significantly higher in the latter. It can be seen that whereas the production rate of the nondecorated cells falls off to almost zero after about 70 h, the decorated bacteria continue producing more vigorously until at least 100 h, with a concomitant increase in DBT → HBP conversion.

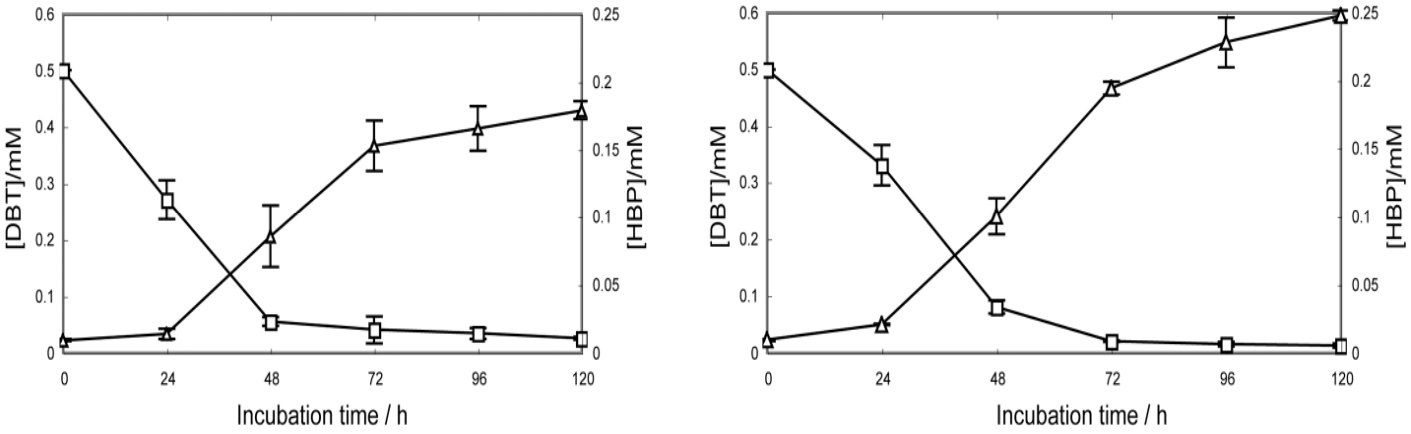

Fig.8. Degradation of DBT by *R. erythropolis* IGTS8 without (left) and with (right) decoration by nanoparticles, in BSM with DBT at the initial (*t* = 0) concentration of 0.5 mM as the sole sulfur source. —□— concentration of DBT, —△— concentration of HBP. The bacteria were present at a concentration of 4×10^7 cm^{-3}.

4. Discussion

The main discovery emerging from these experiments is that the decorated bacteria are significantly more active in desulfurization. Here we discuss possible reasons, starting with the open issue whether the biodesulfurization takes place within the cytoplasm or at the bacterial surface.

4.1 Degradation pathway

The first and rate-limiting step in the oxidative desulfurization of DBT and other sulfur compounds in living organisms is apparently transfer of DBT from the oil to the cell (Setti et al., 1999). In support of this, Folsom et al. (1999) found that the overall rate kinetics were affected by the concentration and distribution of the DBT. It is then oxidized to HBP in several steps by desulfurizing (Dsz) enzymes as illustrated in Scheme 1. These enzymes are

soluble and presumably found in the cytoplasm (Marcelis, 2003). On the other hand, there is no evidence that the DBT molecules are actively transported into the cell (Monticello, 2000). Patel et al. (1997) attributed the mass transfer of the very hydrophobic DBT to the hydrophobic nature of the *Rhodococcus erythropolis* IGTS8 surface, because of their finding that desulfurization activity is correlated to the external surface hydrophobicity of the IGTS8 wall/membrane. It might therefore be supposed that at least some of the enzymes are located in the wall/membrane region[3].

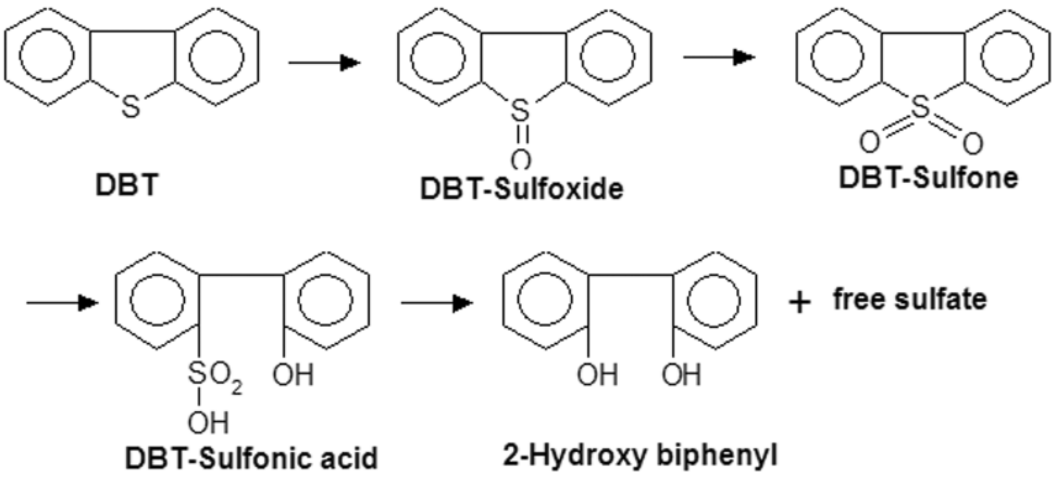

Scheme 1. Proposed (so called 4S) pathway for DBT desulfurization by *R. erythropolis*. The DBT desulfurization pathway results in the formation of 2-hydroxybiphenyl (HBP) and sulfate, via the Dsz enzymes (cf. Van Hamme et al., 2003).

[3] This suggests that some of the desulfurization enzymes should function in nonaqueous solvents, which consequently would facilitate contact with the oil phase and enhance mass transfer during biodesulfurization. In the other words, the *Rhodococcus* strains should be able to access to DBT directly from the oil (Monticello, 2000). This is consistent with the large body of work reporting growth of *R. erythropolis* IGTS8 on hydrocarbons such as hexadecane (Solano et al., 1999).

It is not presently known how the product, HBP, leaves the cells (Monticello, 2000) — assuming it is produced in the cytoplasm, not on the bacterial surface. At any rate the HBP released into the oil maintains fuel value (Gray et al., 1996). However, this compound is toxic to bacterial cells; hence growth and biodesulfurization activity become inhibited by its accumulation (Zhang et al., 2005). The sulfate formed during the 4S pathway remains in the aqueous phase and will combine with any ions — e.g. sodium, ammonium, calcium — that are present in the medium **(**McFarland et al., 1998), and might be assimilated by other microorganisms (Kilbane and Bielaga, 1990).

4.2 Membrane permeabilization

The observation of significantly increased HBP production in the decorated cells suggests that the magnetic nanoparticles somehow facilitate transport of HBP out of the cells — assuming that it is produced in the cytoplasm. A possible mechanism for the enhancement is that the nanoparticles bound to the bacteria make their membranes more permeable. In order to investigate this hypothesis, the possible effect of nanoparticles on membrane permeability was assessed in a model membrane system mimicking the outer bacterial membrane (Grigoriev, 2002). Fig. 9 shows typical results. They provide evidence for nanoparticle-induced permeabilization, supporting the proposed enhanced ingress of DBT into the decorated bacterial cells.

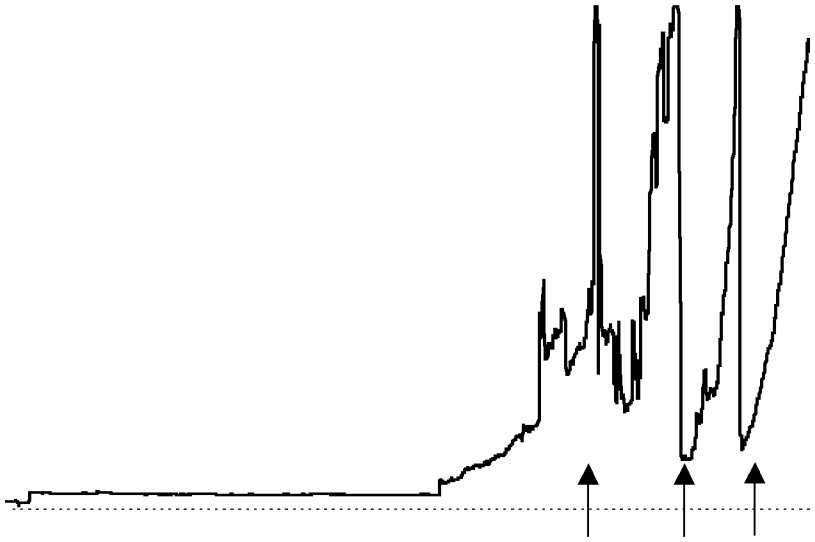

Fig.9. Temporal change of membrane current (ordinate), in the presence of nanoparticles. The sensitivity of the current recording device was changed during the recording (at the moments marked by arrows) from 1 nA/V at the start of the trace to 1 μA/V at the end. Conditions: nanoparticle concentration 300 μg/mL, 200 mM KCl, pH 6, transmembrane voltage 60 mV. The plane of the lipid bilayer was vertical and it was situated about 10 mm above the floor of the glass chamber. Calibrations: vertical 5 pA (initially), horizontal 10 s.

In the model experiments, the added nanoparticles diffuse to the surface of the membrane and are adsorbed. The adsorbed particles diffuse within the membrane, and self-assemble into a conducting transmembrane system, resulting in an increased transmembrane current. Step by step the membrane conductance is increased: it is a dynamic, reversible process, the pore-forming substance can also leave the membrane and the conductance then decreases. The step-like fluctuations of the membrane current at the start of the trace probably correspond to the formation of discrete ion-conducting 20 pS pores.

Table 1. Rate coefficient for biodesulfurization (eqn 1)

	$k / cm^3 s^{-1}$ (means ± s.d.)
Nondecorated	$1.01 \times 10^{-10} \pm 5.92 \times 10^{-12}$
Decorated	$1.58 \times 10^{-10} \pm 6.85 \times 10^{-12}$

4.3 Analysis of the biodesulfurization kinetics

The overall biodesulphurization reaction is:

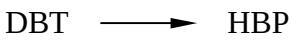

Writing *D* and *H* for the concentrations of DBT and HBP respectively, the corresponding kinetic equation is

$$\frac{dH}{dt} = kDB \qquad (1)$$

where *B* is the concentration of the bacteria and *k* the rate coefficient. The integrated form is

$$\ln\left(1 - \frac{H}{D_0}\right) = -kBt \qquad (2)$$

where D_0 is the initial DBT concentration (0.5 mM). Linear regression of the data from Fig. 8 according to eqn (2) yields *k* (Table 1). It can be seen that decoration increases the biodesulphurization activity by 56%.

5. Conclusions

We decorated bacteria with Fe_3O_4 nanoparticles to facilitate cell separation at the end of the desulfurization process; decoration is facilitated by electrostatic attraction between the nanoparticles and the bacteria. The synthesized nanoparticles are dispersible in water and biological media. Magnetic separation is compatible with any automated platform that can be equipped with a magnet.

We found that we could thereby achieve a 56% higher rate of desulfurization. We favour the view that the rate limiting step of the process is transport of DBT into the cell, where it undergoes desulfurization. We show that the nanoparticles increase the permeability of a model black lipid membrane, and infer that they thereby enhance ingress of the DBT into the cell.

Magnetic nanoparticle- decorated *Rhodococcus* also facilitates its recovery and reuse; hence it offers a number of advantages for industrial applications compared to nondecorated cells. The nanoparticles are easy to prepare from rather cheap precursor materials, and are therefore suitable for large scale industrial applications. The generation of stable, inexpensive and nontoxic adjunct materials for use with microbial cells greatly facilitates the separation of the cells from the products during bioreactor process development, and the removal of the cells from the medium at any time via magnetic decantation.

Acknowledgments

We thank Mimi Hill for the magnetization measurements carried out at Liverpool University and Qi Zhang & Matthew Kershaw (Cranfield University) for help with the zeta potential measurements and XRD respectively.

References

Ansari F, Prayuenyong P, Tothill I. 2007. Biodesulfurization of dibenzothiophene by *Shewanella putrefaciens* NCIMB 8768. J. Biol. Phys. Chem.7:75-78.

Corcoran JA. 1985. The production and use of immobilized living microbial cells. In: Wiseman, A. (Ed.). Topics in Enzyme and Fermentation Biotechnology. England/Ellis Horwood. 10: 12-50.

Gupta PK, Hung CT. 1989. Magnetically controlled targeted micro-carrier systems. Life Sci. 44:175-186.

Díaz MP, Boyd KG, Grigson SJW, Burgess JG, 2002. Biodegradation of crude oil across a wide range of salinities by an extremely halotolerant bacterial consortium MPD-M, immobilized onto polypropylene fibers. Biotechnol. Bioeng. 79:145-153.

Folsom BR, Schieche DR, Digrazia PM, Werner J, Palmer S. 1999. Microbial desulfurization of alkylated dibenzothiophenes from a hydrodesulfurized middle distillate by *Rhodococcus erythropolis* I-19. Appl. Environ. Microbiol. 65:4967-9972.

Gray KA, Pogrebinsky OS, Mrachko GT, Xi L, Monticello DJ, Squires CH. 1996. Molecular mechanisms of biocatalytic desulfurization of fossil fuels. Nat. Biotechnol. 14:1705-1709.

Grigoriev P. 2002. Unified carrier-channel model of ion transfer across lipid bilayer membranes. J. Biol. Phys. Chem. 2:77-79.

Hergt R. Dutz S. Muller R. Zeisberger M. 2006. Magnetic particle hyperthermia: nanoparticle magnetism and materials development for cancer therapy. J. Phys.: Condens. Matter 18:2919–2934.

Hulst AC, Tramper J. 1989. A new technique for the production of immobilized biocatalyst in large quantities. Enzyme Microb. Technol. 11:546-556.

Kayser KJ, Bielaga-Jones BA, Jackowski K, Odusan O, Kilbane JJ. 1993. Utilization of organosulphur compounds by axenic and mixed cultures of Rhodococcus rhodochrous strain IGTS8. J. Gen. Microbiol. 139:3123-3129.

Kilbane JJ, Bielaga BA. 1990. Toward sulfur-free fuels. Chemtech. 20:747-751.

Lee J, Isobe T, Senna M. 1996. Preparation of ultrafine Fe particles by precipitation in the presence of PVA at high pH. J. Colloid Interface Sci. 177:90–494.

Li MZ, Squires CH, Monticello DJ, Childs JD. 1996. Genetic analysis of the dsz promoter and associated regulatory regions of *Rhodococcus erythropolis* IGTS8. Bacteriol. J. 178:6409-6418.

Luo RG, Sirkar KK. 2000. Method and apparatus for isolation purification of biomolecules. US Patent 6,022,477.

Marcelis CLM. 2003. Anaerobic biodesulfurization of thiophenes. PhD Thesis, University of Wageningen.

McFarland BL, Boron DJ, Deever W, Meyer JA, Johnson AR, Atlas RM. 1998. Biocatalytic sulfur removal from fuels: applicability for producing low sulfur gasoline. Crit. Rev. Microbiol. 24:99-147.

Monticello DJ. 2000. Biodesulfurization and the upgrading of petroleum distillates. Curr. Opin. Biotechnol. 11:540-546.

Morrish AH, Yu SP. 1956. Magnetic Measurements on Individual Microscopic Ferrite Particles Near the Single-Domain. Phys. Rev. 102:670-673.

Mueller P, Rudin DO, Tien H, Wescott W. 1962. Reconstitution of cell membrane structure in vitro and its transformation into an excitable system. Nature, 194:979-980.

Naito M, Kawamoto T, Fujino K, Kobayashi M, Maruhashi K, Tanaka A. 2001. Long-term repeated biodesulfurization by immobilized *Rhodococcus erythropolis* KA2-5-1 cells. Appl. Microbiol. Biotechnol. 55:374-378.

Patel SB, KilbaneII JJ, Webster DA. 1997. Biodesulphurisation of dibenzothiophene in hydrophobic media by Rhodococcus sp strain IGTS8. J. Chem. Technol. Biotechnol. 69:100–106.

Prieto MB, Hidalgo A, Serra JL, Llama MJ. 2002. Degradation of phenol by *Rhodococcus erythropolis* UPV-1 immobilized in Biolite in a packed-bed reactor. J. Biotechnol. 97:1-11.

Schmidt H. 2001. Nanoparticles by chemical synthesis, processing to materials and innovative applications. Appl. Organometal. Chem.15:331-343.

Setti L, Farinelli P, Di Martino S, Frassinetti S, Lanzarini G, Pifferi P. 1999. Developments in destructive and non-destructive pathways for selective desulfurizations in oil biorefining processes. Appl. Microbiol. Biotechnol**.** 52:111–117.

Shan G, Xing J, Zhang H, Liu H. 2005. Biodesulfurization of dibenzothiophene by microbial cells coated with magnetic nanoparticles. Appli. Environ. Microbiol. 71:4497-4502.

Solano SF, Marchal R, Ropars M, Lebeault J, Vandecasteele J. 1999. Biodegradation of gasoline: kinetics, mass balance and fate of individual hydrocarbons. J. Appl. Microbiol. 86:1008-1016.

Van Hamme JD, Singh A, Ward OP. 2003. Recent advances in petroleum microbiology. Microbiol. Mol. Biol. Rev. 503-549.

Xu P, Yu B, Li FL, Cai XF, Ma CQ. 2006. Microbial degradation of sulfur, nitrogen and oxygen heterocycles. Trends Microbiol. 14:398-405.

Yang J, Marison WI. 2005. Two-stage process design for the biodesulfurization of a model diesel by a newly isolated *Rhodococcus globerulus* DAQ3. Biochem. Engng 27:77-82.

Yang S, Albayrak N. 2006. Immobilization of enzyme on a fibrous matrix. US Patent 716,6451.

Yeh CS, Cheng FY, Shieh DB, Wu CL. 2004. Method for preparation of water-soluble and dispersed iron oxide nanoparticles and application thereof. US Patent 271,593.

Zhang L, Dong Y, Wang M, Shi S. 2005. Biodesulfurization of dibenzothiophene and other organic sulfur compound by newly isolated *Micobacterium* strain ZD-M2. FEMS Microbiol. Lett. 247:45-50.

Zhang XY, Chen YJ, Fan LN, Li ZY. 2006. Enhancement of low-field magnetoresistance in Fe3O4 particles induced by ball milling. Solid State Comm. 137:673-677.